Follow us @BoneJointRes

Freely available online OPEN ACCESS

BJR

BONE BIOLOGY

Complete abrogation of key osteoclast markers with a membrane-anchored tissue inhibitor of metalloproteinase

A NOVEL APPROACH IN THE PREVENTION OF OSTEOCLASTOGENESIS

Y. Zhang,
B. Jiang,
P. Zhang,
S. K. Chiu,
M. H. Lee

From Xian Jiaotong Liverpool University, Suzhou, China

Aims

Tissue inhibitors of metalloproteinases (TIMPs) are the endogenous inhibitors of the zinc-dependent matrix metalloproteinases (MMP) and A disintegrin and metalloproteinases (ADAM) involved in extracellular matrix modulation. The present study aims to develop the TIMPs as biologics for osteoclast-related disorders.

Methods

We examine the inhibitory effect of a high affinity, glycosyl-phosphatidylinositol-anchored TIMP variant named 'T1^{PrαTACE}' on receptor activator of nuclear factor kappa-B ligand (RANKL)-induced osteoclast differentiation.

Results

Osteoclast progenitor cells transduced with T1^{PrαTACE} failed to form tartrate-resistant acid phosphatase (TRAP)-positive osteoclasts or exhibit bone-resorbing activity following treatment with RANKL. At the messenger RNA level, T1^{PrαTACE} strongly attenuated expression of key osteoclast marker genes that included *TRAP*, *cathepsin K*, osteoclast stimulatory transmembrane protein (*OC-STAMP*), dendritic cell-specific transmembrane protein (*DC-STAMP*), osteoclast-associated receptor (*OSCAR*), and ATPase H^+-transporting V0 subunit d2 (*ATP6V0D2*) by blocking autoamplification of nuclear factor of activated T cells 1 (NFATc1), the osteoclastogenic transcription factor. T1^{PrαTACE} selectively extended p44/42 mitogen-activated protein kinase activation, an action that may have interrupted terminal differentiation of osteoclasts. Inhibition studies with broad-spectrum hydroxamate inhibitors confirmed that the anti-resorptive activity of T1^{PrαTACE} was not reliant on its metalloproteinase-inhibitory activity.

Conclusion

T1^{PrαTACE} disrupts the RANKL-NFATc1 signalling pathway, which leads to osteoclast dysfunction. As a novel candidate in the prevention of osteoclastogenesis, the TIMP could potentially be developed for the treatment of osteoclast-related disorders such as osteoporosis.

Cite this article: *Bone Joint Res* 2022;11(11):763–776.

Keywords: Osteoclasts, Osteoclastogenesis, Cathepsin K, TRAP, TIMP

Article focus

- We aim to develop a tissue inhibitor of metalloproteinases (TIMP) for osteoclast inhibition.
- 'T1^{PrαTACE}' is a glycosylphosphatidylinositol-anchored TIMP capable of blocking osteoclastogenesis.

Key messages

- T1^{PrαTACE} inhibits osteoclastogenesis in osteoclast progenitor cells.
- T1^{PrαTACE} attenuates transcription of multiple key osteoclast markers.

Correspondence should be sent to Meng Huee Lee; email: meng.lee@xjtlu.edu.cn

doi: 10.1302/2046-3758.1111.BJR-2022-0147.R2

Bone Joint Res 2022;11(11):763–776.

- T1^{PrαTACE} blocks autoamplification of master transcription factor nuclear factor of activated T cells 1.

Strengths and limitations

- This is a novel antiosteoclastogenesis strategy that has never been attempted before.
- A broad range of cell- and molecular-based approaches are used to delineate the activities of T1^{PrαTACE}.
- Animal studies are required to assess the potency of the TIMP.

Introduction

Bone homeostasis is a complex balancing act maintained by the coordinated activities of bone-forming osteoblasts and bone-resorbing osteoclasts. Derived from monocytic/macrophagic lineage, osteoclasts are giant multinucleated cells uniquely designed for the dissolution and absorption of bone. During bone remodelling, osteoclast progenitor cells are recruited by osteoblasts to the site of remodelling, wherein macrophage-colony stimulating factor (M-CSF) and receptor activator of nuclear factor-κB (NF-κB) ligand (RANKL) are secreted to initiate osteoclast differentiation.[1] Binding of M-CSF and RANKL to their cognate receptors, colony-stimulating factor-1 receptor (C-FMS) and receptor activator of nuclear factor kappa-β (RANK), prompted osteoclast progenitor cells to commit to osteoclast lineage-specific growth, a cell fusion event mediated by the dendritic cell-specific transmembrane protein (DC-STAMP).[2]

To resorb bone effectively, osteoclasts form ring-shaped adhesion structures known as the "sealing zone" with the underlying bone matrix.[1] It is within the confine of this sealing zone that a number of enzymes, chief among them cathepsin K (CatK), tartrate-resistant acid phosphatase (TRAP), and matrix metalloproteinase (MMP)-9, are secreted to dissolve bone matrix.[1,3] CatK is one of the most prominent cysteine proteinases expressed in osteoclasts of which the primary function is to degrade bone matrix proteins.[4-6] Besides its bone-degrading function, CatK also activates the zymogen of MMP-9, a prominent member of the MMP family whose main function is to degrade and remodel the extracellular matrix, including that of bone.[7] In osteoclasts, MMP-9 is secreted as a latent pro-enzyme that requires activation by CatK in the extracellular space.[7] Mounting evidence indicates that CatK is indispensable for osteoclast-mediated bone resorption, and targeting CatK could offer a promising strategy to prevent osteoclast-related disorders such as osteoporosis.[8]

The aim of the current study is to examine the therapeutic potential of tissue inhibitors of metalloproteinases (TIMPs) in the prevention of osteoclast-mediated bone resorption. As the endogenous inhibitors of the MMPs and A disintegrin and metalloproteinases (ADAMs), TIMPs (TIMP-1 to -4) are small proteins of 21 to 27 kDa in molecular mass.[9] Despite sharing a relatively high degree of sequence homology (40% to 50%), the TIMPs differ vastly in their profiles of metalloproteinase selectivity. For instance, MT1-MMP can be inhibited by TIMP-2, -3, and -4 but not TIMP-1, whereas tumour necrosis factor alpha (TNF-α) converting enzyme (TACE) is selectively inhibited by TIMP-3.[10,11] A recent study carried out on labral tissue with femoroacetabular impingement (FAI) pathology showed an increased expression of MMP-1 and -2, while the level of TIMP-1 was found to be reduced.[12]

In this study, we seek to modulate osteoclast formation and function through a membrane-anchored TIMP variant named 'T1^{PrαTACE}'. T1^{PrαTACE} is a glycosylphosphatidylinositol (GPI)-anchored TIMP mutant originally engineered for the inhibition of TACE.[13,14] We show that T1^{PrαTACE} attenuates RANKL-mediated osteoclast differentiation and bone resorption by preventing nuclear factor of activated T cells (NFATc1) from regulating its own expression. Osteoclast differentiation is fully dependent upon NFATc1,[15] the expression of which is mediated by the binding of RANKL to its receptor RANK which, in turn, triggers p38 mitogen-activated protein kinase (MAPK) phosphorylation.[16] As shown in this study, attenuation in NFATc1 expression abrogates the downstream transcription of key osteoclast marker genes that include *TRAP*, *CatK*, *OC-STAMP,* and *ATP6VD02*. The efficacy of our unique approach may potentially allow for an alternative strategy to be developed for the prevention and treatment of osteoclast-related disorders such as osteoporosis and rheumatoid arthritis.

Methods

Materials. Unless otherwise stated, all the chemicals and reagents used in this study were supplied by Thermo Fisher Scientific (USA). Antibodies for TIMP-1 (Ab1827), TACE (Ab28233), TRAP (Ab191406), CatK (11239 to 1-AP), and NFATc1 (66963 to 1-Ig) were acquired from Abcam (UK), Proteintech (USA), or Novus Biologicals (USA). Osteoclast Identification kit (70-CK20203), TRAP activity test kit (P0332), F-actin staining kit (C2203-S, ActinTracker Red-555), RNeasy Mini Kit (74004), GoScript Reverse Transcription System kit (A5001), and GoTaq qPCR Master Mix kit (A6020) were sourced from MultiSciences (China), Beyotime (China), Qiagen (Germany), and Promega (USA). Enzyme-linked immunosorbent assay (ELISA) kit for TNF-α (10602) was the product of Sino Biological (China). Batimastat (BB-94; S7155), ilomastat (galardin, GM6001; S7157), and TNF-α processing inhibitor (TAPI-0; CAS143457-40-3) were the products of Selleckchem (USA) and Santa Cruz Biotechnology (USA), respectively. Bovine cortical dentin slices (0.2 mm) were purchased from Boneslices (Denmark).

Gelatin zymography, reverse zymography, and ELISA assay kits. Gelatin zymography and reverse zymography were carried out on 10% polyacrylamide gels essentially as described.[17] For MMP-2 and -9 detection, the samples were diluted in phosphate-buffered saline (PBS) prior to loading (25 µl/lane) onto acrylamide gels. All the ELISA assays were performed in triplicate in accordance to the manufacturers' protocols.

Transduction and stable cell line selection. Lentivirus encoding TIMP complementary DNAs (cDNAs) in pLVX vector (Takara, Japan) were transduced in RAW264.7 cells in α-minimum essential medium (α-MEM) supplemented with 8 µg/ml polybrene. For stable cell selection, puromycin (2 µg/ml) was added to the media eight hours post-transduction. To obtain stable cells with the highest fluorescence intensity, the cells were subjected to a second round of selection with fluorescence-activated cell sorting cytometry.

TRAP staining and enzymatic activity assay. To initiate osteoclast formation, RAW264.7 cells in 24-well plates (5,000 cells/well) were induced with RANKL (100 ng/ml) in α-MEM supplemented with 5% fetal bovine serum. At 96 hours following induction, the cells were stained for TRAP and assayed with p-nitrophenyl phosphate (pNPP) for phosphatase activity. TRAP-positive cells with three or more nuclei were identified as osteoclasts. TRAP activity was quantified using a Varioskan colorimetric plate reader (Thermo Fisher Scientific) at 405 nm wavelength. MMP-2, MMP-9, and TNF-α expression were analyzed by gelatin zymography[17] or ELISA.

F-actin ring assays. Cells were fixed and stained with 4% paraformaldehyde/0.1% phalloidin 120 hours after induction with RANKL essentially as described in the product leaflet.

Osteoclast inhibition study with hydroxamate inhibitors. Batimastat, ilomastat, and TNF alpha processing inhibitor-0 (TAPI-0) were added to RAW264.7 cells from low to high concentrations during induction with RANKL. The cells were cultured for days and stained for TRAP.

Reverse transcription-quantitative polymerase chain reaction. Reverse transcription was performed with the GoScript Reverse Transcription System on 1 µg total RNA. Quantitative PCR was performed with the GoTaq qPCR Master Mix kit on a Thermo QuantStudio 5 Real-Time PCR System as follows: initial denaturation at 95°C for five minutes; 40 cycles of denaturation at 95°C for 15 seconds; and annealing/extension of product at 60°C for 60 seconds. Relative gene expression was calculated using the comparative C_t method and presented as the messenger RNA (mRNA) level relative to that of the glyceraldehyde 3-phosphate dehydrogenase (GAPDH) gene. Three replicates were performed for each RNA sample. Primer information is provided in Supplementary Table i.

Immunofluorescence microscopy. Cells in Nunc Lab-Tek II chamber slides were fixed, blocked, and permeabilized with 5% bovine serum albumin/0.3% Triton X-100 in PBS for two hours. Following incubation in primary antibodies at 4°C overnight, the cells were rinsed and probed with Alexa Fluor-conjugated secondary antibodies prior to visualization with a Zeiss LSM880 Airyscan confocal microscope (Germany).

Bone resorption pit assay. RAW264.7 cells (3×10^3 cells per well) transduced with wild-type TIMP-1 or T1^{PrαTACE} were seeded on bovine cortical dentin slices and incubated for 21 days in α-MEM supplemented with 100 ng/ml RANKL (n = 4). Following gentle sonication and brushing, the bone slices were stained with 1% toluidine blue before images were taken and quantified for bone resorption using ImageJ software (USA).

Statistical analysis. Statistical analysis between subgroups was carried out with the paired *t*-test or analysis of variance (ANOVA) using Social Science Statistics. All data are presented as the means of three experimental repeats and standard deviation (SD). Only p-values < 0.05 were considered as statistically significant. To ensure the reproducibility of the results, all the experiments that required quantification had been performed on at least three biological replicates for a minimum of three times.

Results

T1^{PrαTACE}: a GPI-anchored TIMP engineered for the inhibition of TACE. Listed in Figure 1a are the amino acid sequences for the wild-type TIMP-1 (T1), a GPI-linked TIMP-1 'T1^{Pr}' and a GPI-linked TIMP-1 variant 'T1^{PrαTACE}' engineered for the inhibition of TACE. As shown by Lee et al,[14] T1^{PrαTACE} is a high-affinity TIMP-1 variant that has undergone extensive mutation at the MMP-binding ridge (K_i^{app} for TACE 0.14 nM). Immunofluorescence (IF) study performed on RAW264.7 progenitor cells showed intense membrane staining in cells transduced with T1^{Pr} and T1^{PrαTACE}, but not the wild-type TIMP-1 (Figure 1b). Additional reverse zymography and immunoblotting studies confirmed the sequestration of T1^{Pr} and T1^{PrαTACE} to the membrane extracts as anticipated (Figure 1c).

We next assessed the potency of T1^{PrαTACE} against TACE. While wild-type TIMP-1 and T1^{Pr} exhibited only a partial degree of inhibitory potency, T1^{PrαTACE} reduced TNF-α shedding by > 90% (Figure 1d). The data showed that T1^{PrαTACE} was a functional and effective inhibitor against TACE enzyme. Despite the potency, T1^{PrαTACE} appeared to have little effect on the expression of TACE protein (Figure 1e).

T1^{PrαTACE} suppressed RANKL-mediated osteoclast differentiation and bone resorption. While the majority of the osteoclasts from the control, wild-type TIMP-1, and T1^{Pr} groups were > 200 µm in diameter, far fewer osteoclasts were observed in T1^{PrαTACE} cells (Figure 2a; Supplementary Figure a). Formation of F-actin rings represents a hallmark for osteoclast differentiation.[18] A complementary staining study performed using phalloidin showed a 93% decrease in the number of F-actin rings in T1^{PrαTACE} cells (Figure 2b, Supplementary Figure a). We next examined if T1^{PrαTACE} could prevent osteolytic bone resorption on bovine cortical dentin slices. A significant decrease (> 80%) in TRAP staining and area of resorption could be visualized in the cells transduced with T1^{PrαTACE}, but not wild-type TIMP-1 ($p < 0.001$, paired *t*-test) (Figures 3a and 3b).

T1^{PrαTACE} inhibited expression of TRAP and MMP-9 maturation. RAW264.7 progenitor cells transduced with T1^{PrαTACE} exhibited a far lower level of TRAP staining (> 90%) and enzymatic activity upon induction with RANKL (Figure 4a).

Besides TRAP, exposure to RANKL also induced a marked increase in MMP-9, but not MMP-2, during

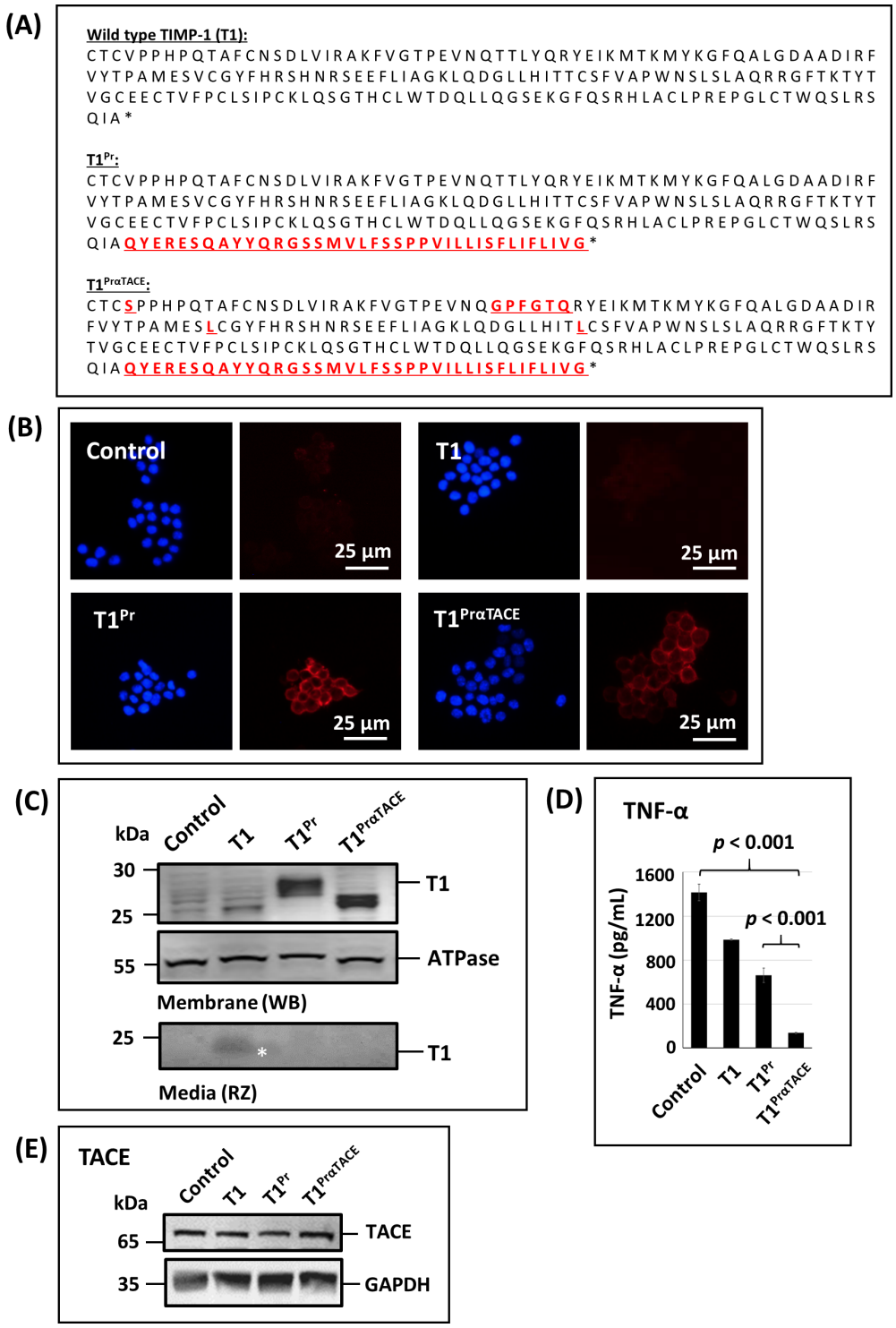

Fig. 1

T1PrαTACE: a high affinity, glycosylphosphatidylinositol (GPI)-tethered tissue inhibitor of metalloproteinases (TIMP) engineered for the inhibition of tumour necrosis factor-α converting enzyme (TACE). a) Amino acid sequences for the wild-type TIMP-1 (T1; top); GPI-tethered TIMP-1 (T1Pr; middle); and a GPI-tethered TIMP variant named 'T1PrαTACE' (bottom). Originally tailored for the inhibition of the A disintegrin and metalloproteinases (ADAM) proteinases, T1PrαTACE has a higher affinity (K_i^{app} 0.14 nM (standard deviation (SD) 0.06)) for TACE than the wild-type TIMP-1 (356 nM (SD 87)).[13,14] b) Membrane localization of GPI-anchored T1Pr and T1PrαTACE in RAW264.7 cells as shown by non-permeabilized immunofluorescence (IF). Intense membrane staining was detected only in the cells transduced with T1Pr and T1PrαTACE (blue, 4′,6-diamidino-2-phenylindole (DAPI)-stained nucleus; red, TIMP staining). c) Sequestration of T1Pr and T1PrαTACE to the cell membrane as shown by reverse zymography and immunoblotting of the membrane extracts and conditioned media. The presence of wild type TIMP-1 in the conditioned media is highlighted by asterisk (*). RZ, reverse zymography; WB, western blot. d) T1PrαTACE was a potent inhibitor of TACE that reduced TNF-α shedding by > 90%. e) T1PrαTACE had a negligible effect on the expression of TACE protein. GAPDH, glyceraldehyde 3-phosphate dehydrogenase. Statistical significance between different groups was determined by analysis of variance.

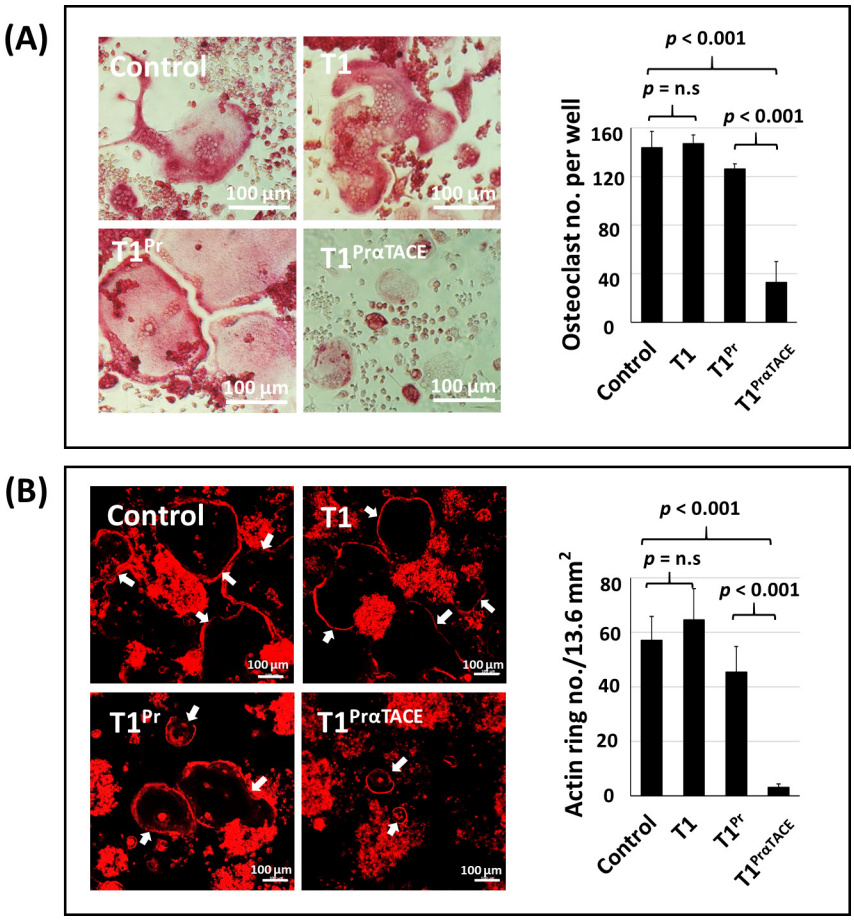

Fig. 2

T1^{PrαTACE} abrogated receptor activator of nuclear factor kappa-B ligand (RANKL)-mediated osteoclast differentiation. a) RAW264.7 cells transduced with T1^{PrαTACE} were not able to transform into osteoclasts in response to RANKL induction. Left: tartrate-resistant acid phosphatase (TRAP)-stained multinucleated osteoclasts 120 hours after induction with RANKL. Right: A significantly lower number of osteoclasts was observed in RAW264.7 cells transduced with T1^{PrαTACE}. b) Phalloidin-stained F-actin rings characteristic of bone-resorbing osteoclasts. In marked contrast to the larger and more irregularly-shaped F-actin rings in the wild-type T1 and T1^{Pr} groups, far fewer F-actin rings were detected in T1^{PrαTACE} cells. Osteoclasts are highlighted by arrows. Statistical significance was determined by analysis of variance. n. s., not significant.

osteoclast differentiation (Figure 4b). Of note, MMP-9 produced by T1^{PrαTACE} cells remained mostly in latent form (102 kDa), which migrated at a slightly slower pace than matured MMP-9 (92 kDa) in a non-reducing zymography gel (Figure 4b).[19] The findings confirmed that pro-MMP-9 was not able to be processed to the matured form in T1^{PrαTACE} cells.

Complete abrogation of CatK expression in T1^{PrαTACE}-transduced cells. Figure 5a summarizes the immunoblot profile of CatK in differently transduced RAW264.7 cells 120 hours post-induction with RANKL. While CatK expression increased dramatically in the control, T1, and T1^{Pr} cells upon induction with RANKL, no CatK could be detected in T1^{PrαTACE}. Time course analysis showed that CatK protein appeared in the control cells 72 hours following exposure to RANKL, and remained stable until the end of the experiment at 120 hours. In contrast, no CatK could be identified in T1^{PrαTACE} throughout the entire course of this study (Figure 5b). The findings were supported by IF microscopy results, which revealed a complete absence of CatK in T1^{PrαTACE} cells that had been RANKL-induced for 120 hours (Figure 5c).

T1^{PrαTACE} suppressed the mRNA expression of osteoclast-specific marker genes. To elucidate the effects of T1^{PrαTACE} at the genetic level, real-time reverse transcription quantitative polymerase chain reaction (RT-qPCR) was performed on osteoclast-specific marker genes including *CatK*, *TRAP*, *DC-STAMP*, osteoclast stimulatory transmembrane protein (*OC-STAMP*), ATPase H^+-transporting V0 subunit d2 (*ATP6V0D2*), and osteoclast-associated receptor (*OSCAR*). Also included in the study was *NFATc1*, the master transcription factor that regulates terminal osteoclast differentiation. Transcriptional activities of CatK and OC-STAMP were found to be abrogated to pre-induction level in T1^{PrαTACE} (Figure 6). For TRAP and ATP6V0D2, at least 60% reduction in the mRNA levels was noted in T1^{PrαTACE}. DC-STAMP and OSCAR were the least affected as only a moderate 25% to 30% downregulation was observed in their mRNA contents. Overall, the data were in agreement with the findings from previous TRAP staining and

Figure 3

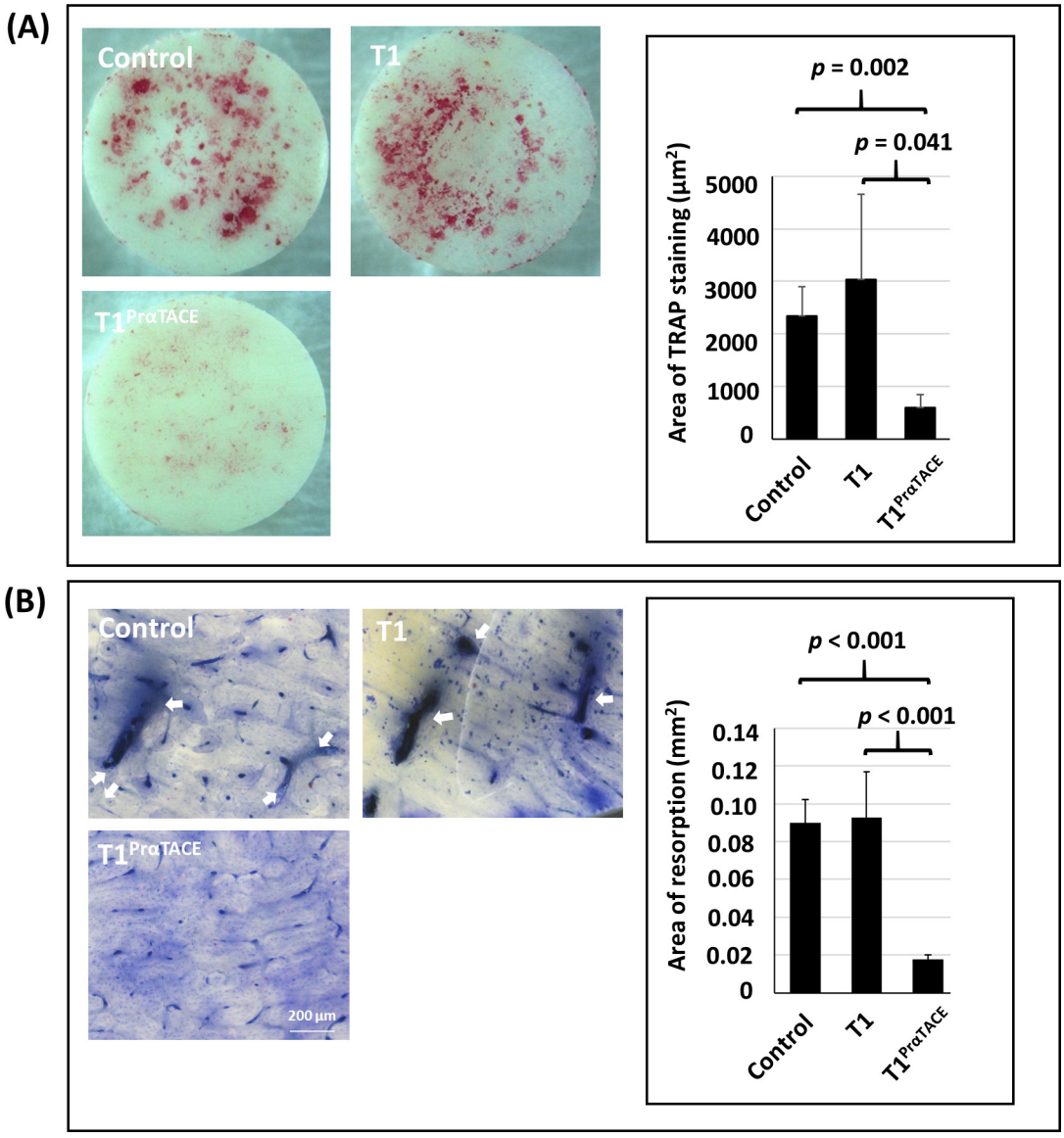

Fig. 3

T1^{PrαTACE} suppressed osteolytic bone resorption on bovine cortical dentin slices. RAW264.7 cells transduced with wild-type tissue inhibitor of metalloproteinases (TIMP)-1 or T1^{PrαTACE} were cultured on bovine cortical dentin slices for 21 days in 100 ng/ml receptor activator of nuclear factor kappa-B ligand. A clear reduction in a) tartrate-resistant acid phosphatase (TRAP) staining and b) bone resorption (> 80%) can be visualized in T1^{PrαTACE} cells following staining with toluidine (n = 4). Resorption pits and trenches on dentin slices are highlighted by arrows. p-values were calculated using analysis of variance.

immunoblotting studies (Figures 4 and 5). Consistent with the zymography results (Figure 4b), no significant alteration in the mRNA expression of MMP-9 gene was detected in T1^{PrαTACE}. A finding of particular interest was the near-complete abrogation of NFATc1 mRNA in T1^{PrαTACE}.

T1^{PrαTACE} prevented NFATc1 from autoregulating its own expression. Next, we probed the protein expression of NFATc1 in osteoclast progenitor cells transduced with different TIMP variants. A > 98% reduction in NFATc1 protein was observed in the cells that had been transduced with T1^{PrαTACE}, but not the other TIMPs (Figure 7a). Time course analysis revealed that NFATc1 was more readily degraded in T1^{PrαTACE} cells, as evidenced from the multiple lower molecular weight bands on the immunoblots (Figure 7b). The findings were corroborated by IF study, which revealed a marked reduction of NFATc1 in T1^{PrαTACE} cells that had been subjected to RANKL induction for 120 hours (Figure 7c).

We next examined nuclear translocation of NFATc1 in the cells that had been induced with RANKL for 24 hours.

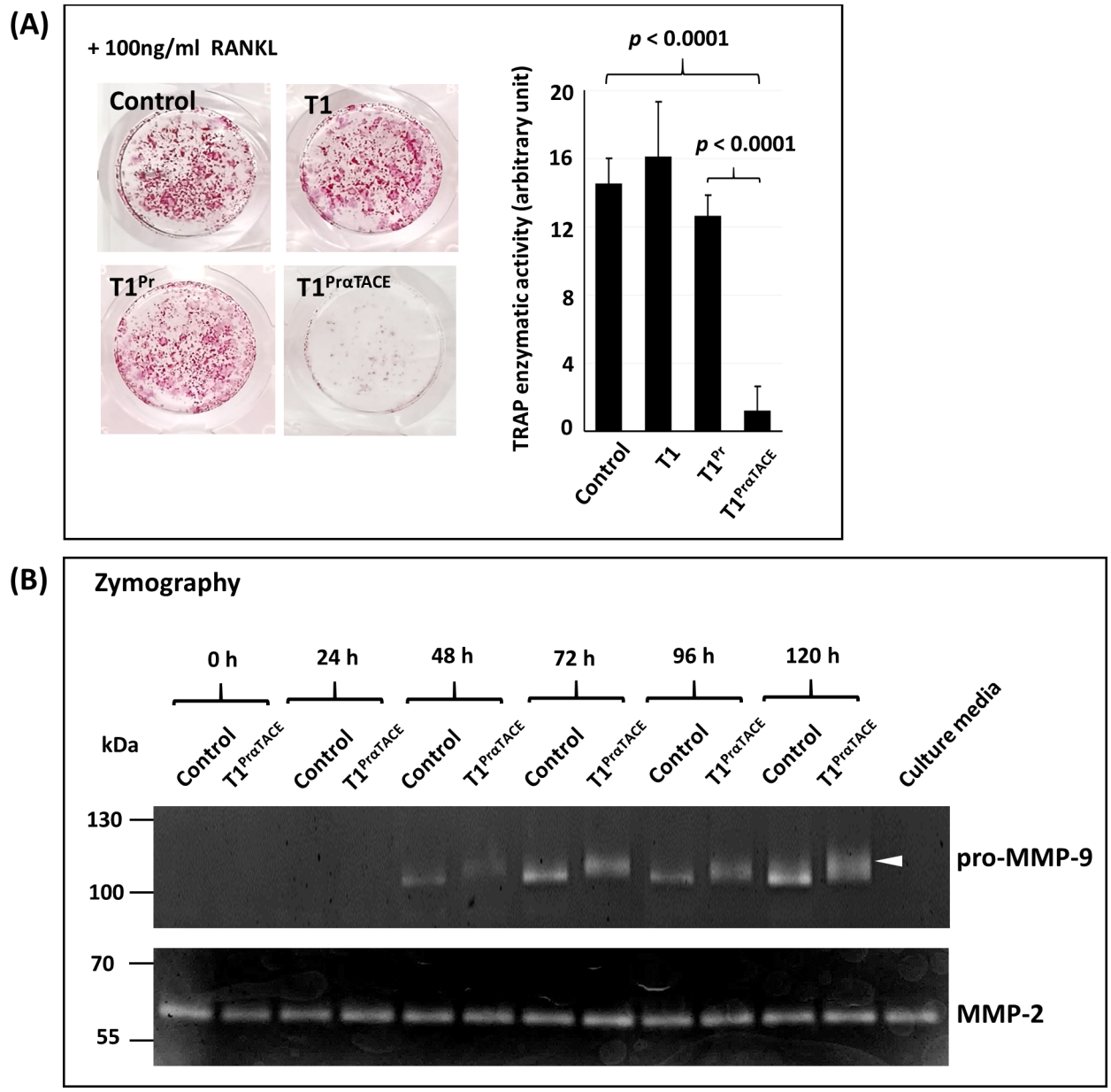

Fig. 4

T1^{PrαTACE} inhibited tartrate-resistant acid phosphatase (TRAP) expression and matrix metalloproteinase (MMP)-9 maturation in osteoclast progenitor cells. a) RAW264.7 progenitor cells transduced with T1^{PrαTACE} exhibited a > 90% lower TRAP staining (left) and activity (right) than the other tissue inhibitor of metalloproteinases (TIMP) variants. b) Gelatin zymography analysis of the conditioned media revealed that MMP-9 expressed in T1^{PrαTACE} cells existed mainly in a zymogen form (102 kDa; highlighted by arrowhead), which migrated at a slower pace than matured MMP-9 (92 kDa). Note: the MMP-2 band in the culture media (last lane) originated from fetal bovine serum added to α-minimum essential medium (5%). RANKL, receptor activator of nuclear factor kappa-B ligand. Statistical significance was determined by analysis of variance.

NFATc1 was clearly visible within the nuclei of both the control and T1^{PrαTACE} cells, confirming that nuclear translocation of NFATc1 was unaffected by T1^{PrαTACE} at least during the early phase of osteoclast differentiation (Figure 7d).

To gain further insight into how T1^{PrαTACE} interfered with the transcriptional profile of NFATc1, we quantitated the NFATc1 mRNA at 0, 24 hours, 48 hours, 72 hours, and 120 hours following treatment with RANKL. The results agreed with the findings from the immunoblot study, in that NFATc1 mRNA underwent decay more rapidly in the cells that expressed T1^{PrαTACE}. Despite an early moderate induction at 24 hours, the level of NFATc1 mRNA in T1^{PrαTACE} cells was rapidly reduced to that of the pre-induction level by 120 hours (Figure 7e). Overall, the transcriptional activity of NFATc1 in T1^{PrαTACE} was far lower than that of the control cells. The findings confirmed that T1^{PrαTACE} prevented NFATc1 from sustaining its own transcription, a process crucial for the lengthy process of osteoclast differentiation.

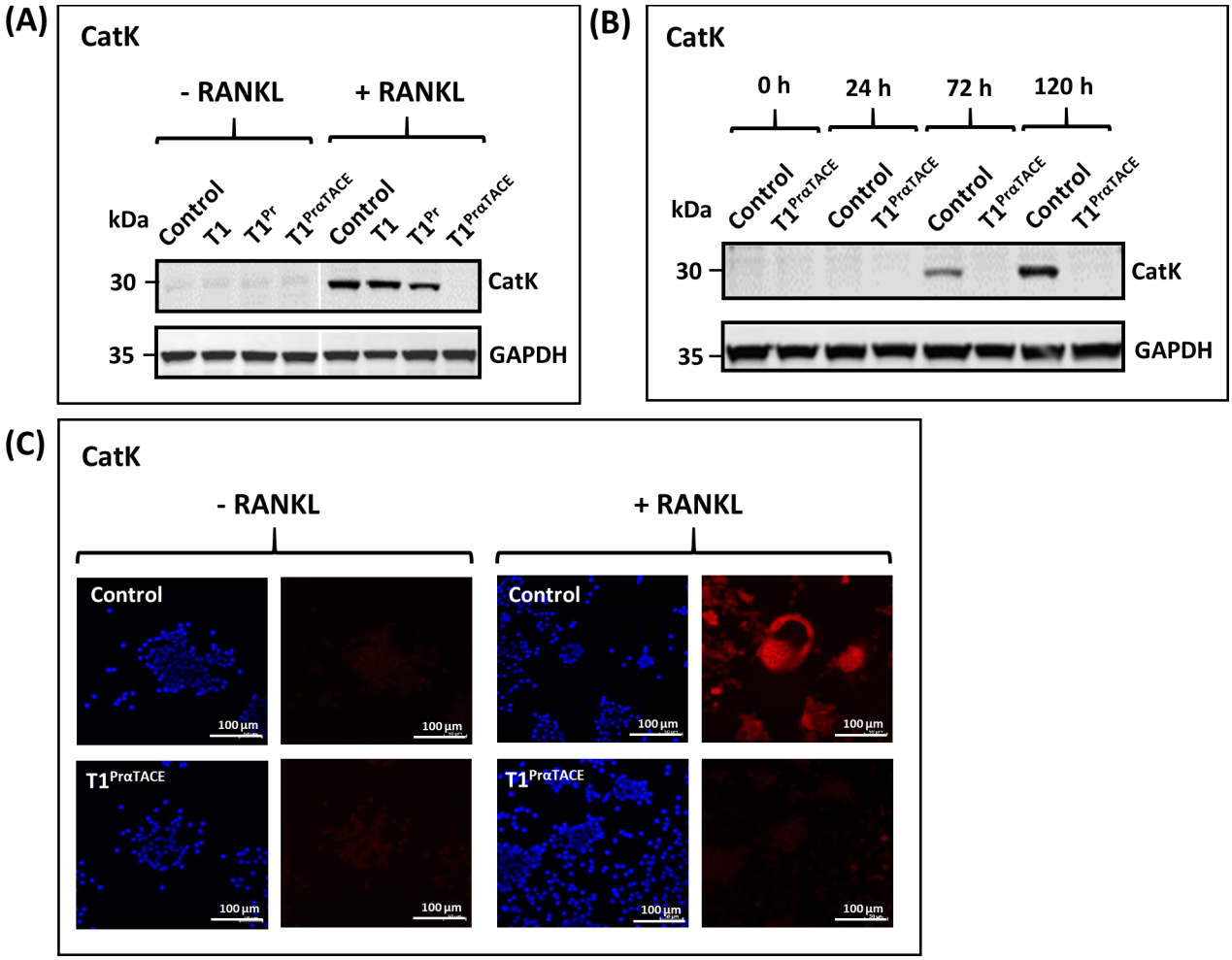

Fig. 5

Complete abrogation of cathepsin K (CatK) expression by T1^{PraTACE}. a) CatK was not detectable in T1^{PraTACE} as shown by immunoblotting of the cell lysates 120 hours after induction with receptor activator of nuclear factor kappa-B ligand (RANKL). b) Time course analysis over 120 hours revealed the absence of CatK in T1^{PraTACE} cells. c) Immunofluorescence (IF) staining shows the absence of CatK in RANKL-induced T1^{PraTACE} cells (blue: 4′,6-diamidino-2-phenylindole staining of the nucleus; red: IF staining of CatK; ×200 magnification). GAPDH, glyceraldehyde 3-phosphate dehydrogenase.

T1^{PraTACE} induced sustained activation of p44/42 MAPK to inhibit NFATc1 autoamplification. To examine the effects T1^{PraTACE} has on RANK protein and MAPK signalling pathways, we next subjected the cell lysates to immunoblotting with p38 and p44/42 antibodies. The results confirmed that, whereas expression of RANK and phosphorylation of p38 MAPK remained relatively unchanged, the level of phosphorylated p44/42 MAPK was more intense and longer-lasting in cells transduced with T1^{PraTACE} (Figures 8a and 8b). Of note, residual expression of phosphorylated p44/42 MAPK was detectable in T1^{PraTACE} even after 24 hours of induction.

T1^{PraTACE} was unique in abrogating osteoclastogenesis. To investigate if T1^{PraTACE} was unique in suppressing osteoclastogenesis, two mutants of different biophysical characteristics were created: 1) T1$^{\alpha TACE}$, a soluble TIMP mutant with the same sequence as that of T1^{PraTACE} except the GPI anchor; and 2) T1^{PraMT1}, a GPI-anchored TIMP mutant designed specifically for the inhibition of MT1-MMP (K_i^{app} 1.66 ± 0.17 nM for MT1-MMP)[20,21] (Figure 9a). Reverse zymography and immunoblotting studies confirmed that T1$^{\alpha TACE}$ was highly soluble, whereas T1^{PraMT1} was sequestered to the membrane fraction (Supplementary Figure b). Despite sharing similar sequences as T1^{PraTACE}, T1$^{\alpha TACE}$ and T1^{PraMT1} were not able to suppress TRAP expression, thus confirming the uniqueness of T1^{PraTACE} as a negative regulator of osteoclastogenesis (Figure 9b).

The anti-osteoclastogenic potency of T1^{PraTACE} was not related to its metalloproteinase-inhibitory activities. To explore if RANKL-mediated osteoclastogenesis required the proteolytic activities of MMPs and TACE, batimastat (a broad spectrum inhibitor active against the MMPs and TACE), ilomastat (a mainly MMP inhibitor), and TAPI-0 (a TACE inhibitor) were added to the cells during the induction process (0.5 to 10 µM). None of the inhibitors were able to prevent osteoclast differentiation irrespective of their concentrations (Figure 9c). The results confirmed that T1^{PraTACE} attenuated osteoclastogenesis via a

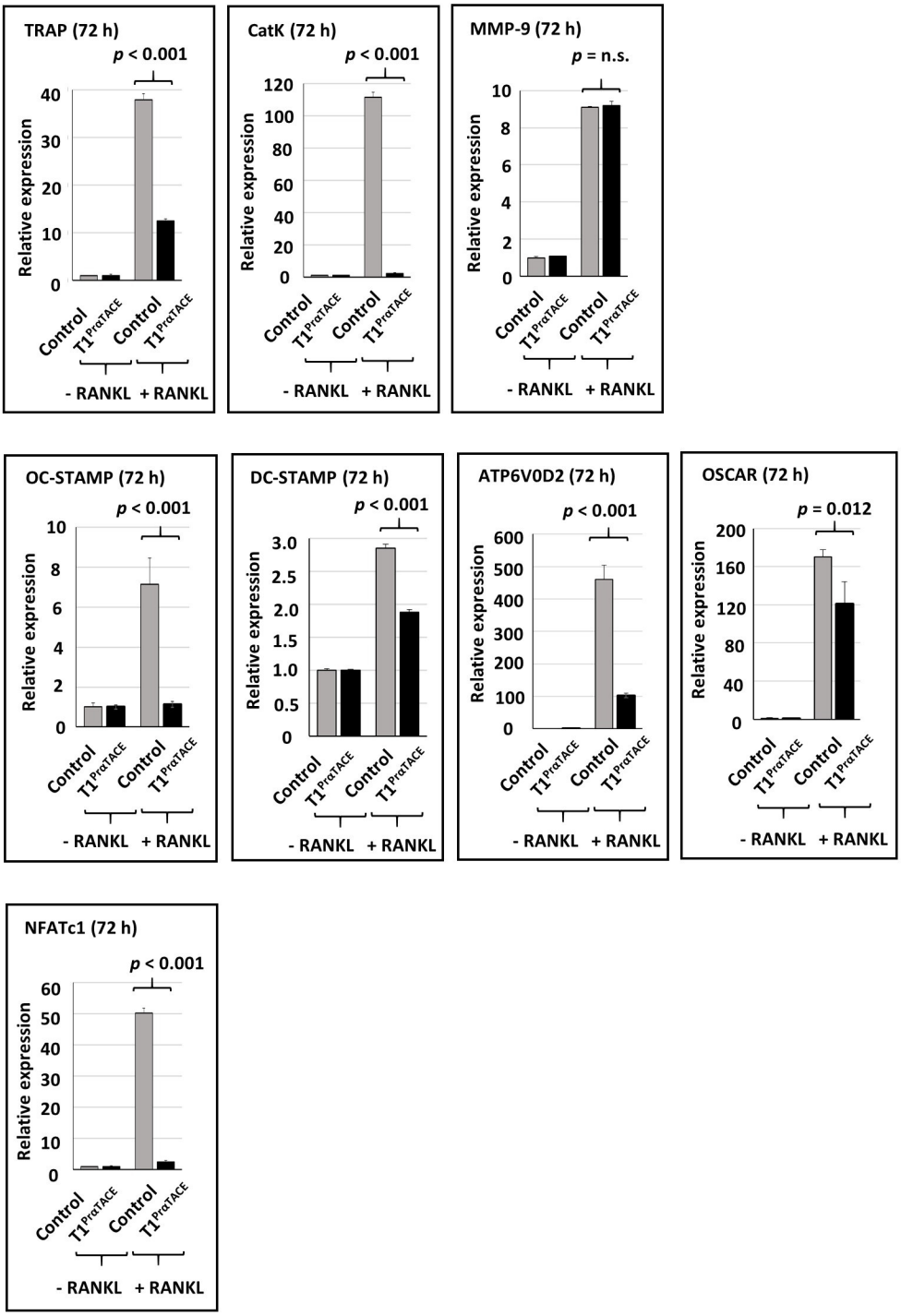

Fig. 6

T1^{PrαTACE} downregulated a broad range of key osteoclast genes. Reverse transcription quantitative polymerase chain reaction analysis revealed a marked downregulation of key osteoclast-specific genes tartrare-resistant acid phosphatase (*TRAP*), cathepsin K (*CatK*), osteoclast stimulatory transmembrane protein (*OC-STAMP*), dendritic cell-specific transmembrane protein (*DC-STAMP*), ATPase H^+-transporting V0 subunit d2 (*ATP6V0D2*), and osteoclast-associated receptor (*OSCAR*) in T1^{PrαTACE} cells. A 98% decrease in messenger RNA (mRNA) expression was also revealed in nuclear factor of activated T cells 1 (*NFATc1*). In contrast, no significant change was detected in the level of matrix metalloproteinase (MMP)-9 mRNA, thus corroborating the findings of the zymography study in Figure 4b. n.s., not significant; RANKL, receptor activator of nuclear factor kappa-B ligand. P-values were calculated using paired *t*-test.

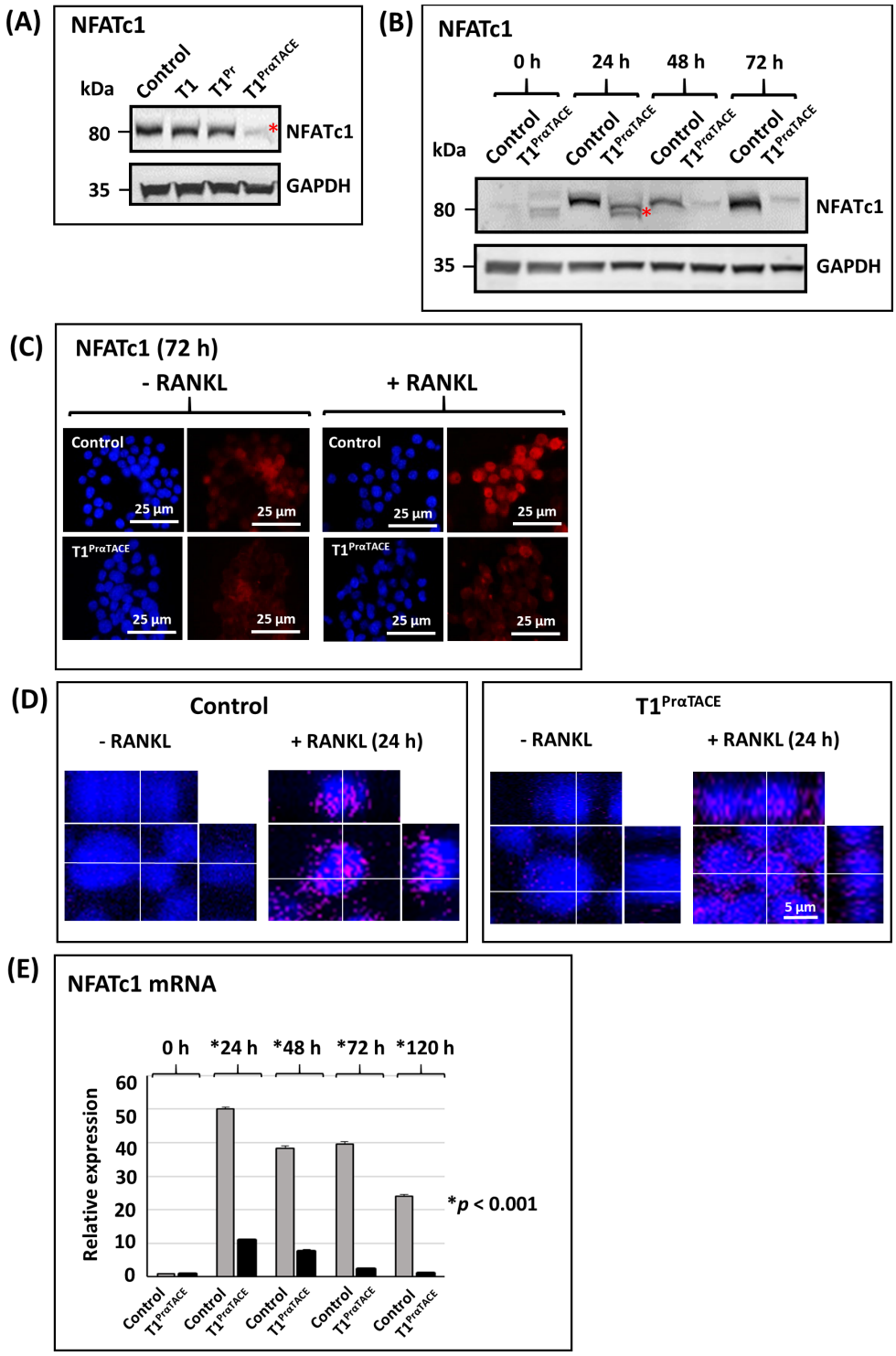

Fig. 7

T1PrαTACE prevented nuclear factor of activated T cells 1 (NFATc1) autoamplification required for the process of osteoclast differentiation. a) A > 98% downregulation in NFATc1 protein (highlighted by asterisk *) was detected in RAW264.7 cells transduced with T1PrαTACE 72 hours after induction with receptor activator of nuclear factor kappa-B ligand (RANKL) (quantification with ImageJ (National Institutes of Health, USA)). b) NFATc1 was more susceptible to degradation in T1PrαTACE as evidenced from the multiple lower molecular weight bands on the immunoblot (highlighted by asterisk *). c) Immunofluorescence (IF) staining revealed a lower expression of NFATc1 in T1PrαTACE cells 72 hours post-induction with RANKL (blue colour: 4′,6-diamidino-2-phenylindole (DAPI) staining of the nucleus; red colour: IF staining of NFATc1). d) T1PrαTACE had no effect on nuclear translocation of NFATc1. Orthogonal views captured with a confocal microscope showing nuclear translocation of NFATc1 in control and T1PrαTACE cells induced with RANKL for 24 hours (blue colour: DAPI staining of the nucleus; red colour: IF staining of NFATc1). e) T1PrαTACE prohibited NFATc1 from sustaining its own transcription. Reverse transcription quantitative polymerase chain reaction quantification of NFATc1 messenger RNA (mRNA) at 0 hrs, 24 hrs, 48 hrs, 72 hrs, and 120 hrs after treatment with RANKL. Despite an early induction at 24 hours, the level of NFATc1 mRNA in T1PrαTACE was rapidly reduced to that of the pre-induction level by 120 hours. Statistical significance was determined by paired *t*-test.

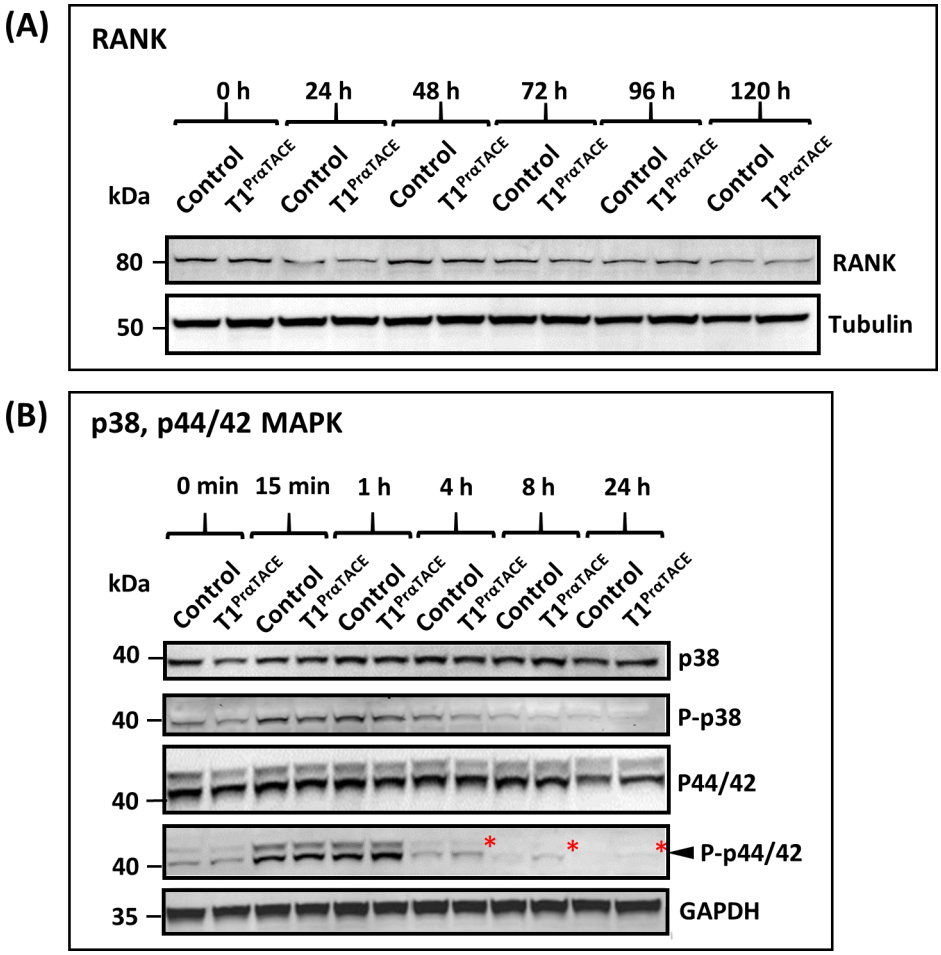

Fig. 8

Selective and sustained activation of p44/42 mitogen-activated protein kinase (MAPK) in T1^{PrαTACE} cells in response to receptor activator of nuclear factor kappa-B ligand (RANKL) induction. a) T1^{PrαTACE} had a negligible effect on the protein expression of RANK throughout the process of osteoclastogenesis. b) Selective and sustained activation of p44/42 MAPK in T1^{PrαTACE} cells. Note the residual expression of phosphorylated p44/42 (highlighted by asterisk *), but not p38 MAPK, in T1^{PrαTACE} cells even after 24 hours of induction. P-p38 and P-p44/42 denote the phosphorylated forms of p38 and p44/42 MAPKs, respectively.

mechanism unrelated to its metalloproteinase-inhibiting activities.

Discussion

Uncontrolled osteoclastogenesis results in increased susceptibility to bone fractures and pathological diseases such as Paget's disease and osteoporosis.[3] Designing novel drugs that target RANKL–RANK interaction and the immediate downstream signalling cascades could potentially revolutionize future pharmacological treatment of many diseases associated with bone loss including osteoporosis, arthritis, and bone cancers. Among the osteoclast-specific gene markers, CatK and TRAP are the most studied due to their critical involvement in bone restructuring.[22,23]

Our strategy to prevent bone resorption with TIMPs is novel and hitherto unattempted. In this study, we demonstrate that osteoclastogenesis was inhibited at both the transcriptional and translational levels by T1^{PrαTACE}. The fact that none of the hydroxamate inhibitors were able to prevent osteoclast differentiation indicates that the antiosteoclastogenic activity of T1^{PrαTACE} is unrelated to its metalloproteinase-inhibitory activity. A finding of particular interest was the selectivity of T1^{PrαTACE} in prolonging p44/42 MAPK activation. NFATc1 production can be induced by activating MAPKs such as p38 and p44/42 (also known as extracellular signal-regulated kinase) through the binding of RANKL to RANK.[24] Interestingly, constitutive activation of p44/42 MAPK has been shown to impede osteoclast differentiation.[25,26] In the case of Yi et al,[26] a neutralizing antibody to CD9 was able to suppress RANKL-mediated osteoclastogenesis by inducing a stronger and longer p44/42 phosphorylation. This selective activation of MAPK was similar to the effect of T1^{PrαTACE} we observed in this study. We surmised that the failure of T1^{PrαTACE} cells in undergoing osteoclast differentiation could be attributed, at least in part, to the effect of TIMP on p44/42 MAPK phosphorylation. We are currently identifying the molecular mechanism

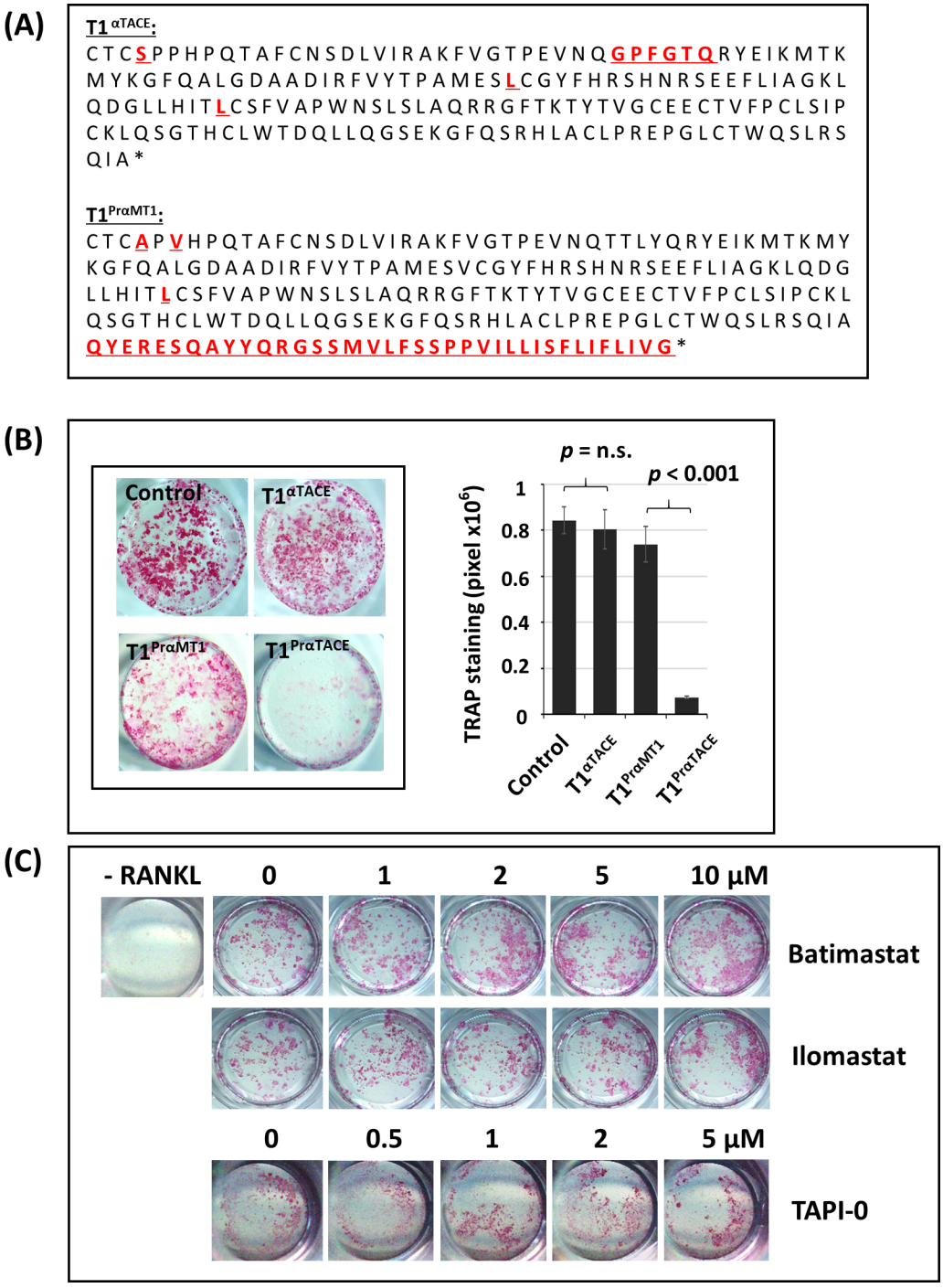

Fig. 9

T1PrαTACE was unique as a negative regulator of osteoclastogenesis. a) Amino acid sequences for T1αTACE and T1PrαMT1. T1αTACE was a soluble tissue inhibitor of metalloproteinases (TIMP) that bore the same amino acid sequence as T1PrαTACE except for the glycosylphosphatidylinositol (GPI) signal peptide. T1PrαMT1 was a GPI-anchored TIMP-1 variant designed specifically for the inhibition of MT1-matrix metalloproteinase (MMP).[20,21] b) Despite sharing similar sequences with T1PrαTACE, T1αTACE and T1PrαMT1 were unable to inhibit osteoclast differentiation. c) None of the hydroxamate inhibitors batimastat (a broad-spectrum inhibitor active against MMPs and tumour necrosis factor-α converting enzyme (TACE)), ilomastat (a mainly MMP inhibitor), and TNF alpha processing inhibitor-0 (TAPI-0) (a TACE inhibitor) were able to inhibit receptor activator of nuclear factor kappa-B ligand (RANKL)-mediated osteoclast differentiation. The data confirmed that the potency of T1PrαTACE was derived from a mechanism independent of its metalloproteinase-inhibitory activity. n.s., not significant.

underlying T1^{PrαTACE}/p44/42 MAPK signalling cascade(s) that led to an abrogation in NFATc1 autoamplification.

Based on the findings here, we can conclude that T1^{PrαTACE} inhibits RANKL-mediated osteoclast differentiation primarily by preventing NFATc1 autoregulation. Acting possibly by prolonging p44/42 MAPK phosphorylation, T1^{PrαTACE} blocked NFATc1 from regulating its own expression. As the key transcriptional regulator pivotal for osteoclast differentiation, NFATc1 upregulates a broad range of osteoclast-specific markers that include TRAP, CatK, DC-STAMP, OC-STAMP, ATP6V0D2, and OSCAR.[27-29] CatK in particular is renowned for its dual abilities in bone resorption and MMP-9 activation.[7] As in the case of T1^{PrαTACE}, a depletion in NFATc1 leads to an abrogation of these markers and a functionally incapacitated osteoclast progenitor cell that failed to carry out MMP-9 activation or undergo cell fusion in response to RANKL induction.

NFATc1 also mediates MMP-9 transcription.[27] Our data showed that MMP-9 transcription was not adversely affected by the downregulation in NFATc1. The failure of T1^{PrαTACE} to abrogate MMP-9 transcription suggests that the signalling mechanism that regulates MMP-9 production during osteoclast differentiation is likely to be different from that for TRAP and CatK. TNF-α potentiates osteoclast differentiation by upregulating osteoclastogenic cytokines M-CSF and RANKL in osteoblast-like cells.[30] As a potent TACE inhibitor, T1^{PrαTACE} is on its own capable of blocking the release of TNF-α to further diminish the occurrence of osteoclastogenesis potentiated via the TNF-α pathway.

In conclusion, we have presented here concrete evidence to demonstrate the efficiency of T1^{PrαTACE} as a lead biologic in the suppression of osteoclastogenesis. By incorporating T1^{PrαTACE} into a delivery platform such as adeno-associated virus, we hope to develop the TIMP into a medicine suitable for the treatment of diseases characterized by osteoclast hyperactivity. An alternative approach would be to incorporate T1^{PrαTACE} into the genome of the target cells using gene editing tools such as clustered regularly interspaced short palindromic repeats (CRISPR) for a more personalized, bespoke treatment.[31] In addition to this, we are investigating the mechanism by which T1^{PrαTACE} disrupts RANKL-RANK signalling cascades using immunoprecipitation and different omics approaches. The data presented in this study have provided us with new insights into the pathogenesis of osteoclastogenesis and possibly new strategies for antiresorptive drug development.

Supplementary material

Table of polymerase chain reaction (PCR) primers used for quantifying osteoclast marker gene expression by reverse transcription (RT)-qPCR; figures showing results of tartrate-resistant acid phosphatase and phalloidin staining, and reverse zymography and immunoblotting.

References

1. **Takito J**, **Inoue S**, **Nakamura M**. The sealing zone in osteoclasts: A self-organized structure on the bone. *Int J Mol Sci*. 2018;19(4):E984.
2. **Chiu YH**, **Ritchlin CT**. DC-STAMP: A key regulator in osteoclast differentiation. *J Cell Physiol*. 2016;231(11):2402–2407.
3. **Bi H**, **Chen X**, **Gao S**, **et al**. Key triggers of osteoclast-related diseases and available strategies for targeted therapies: A review. *Front Med (Lausanne)*. 2017;4:234.
4. **Bossard MJ**, **Tomaszek TA**, **Thompson SK**, **et al**. Proteolytic activity of human osteoclast cathepsin K. Expression, purification, activation, and substrate identification. *J Biol Chem*. 1996;271(21):12517–12524.
5. **Garnero P**, **Borel O**, **Byrjalsen I**, **et al**. The collagenolytic activity of cathepsin K is unique among mammalian proteinases. *J Biol Chem*. 1998;273(48):32347–32352.
6. **Kafienah W**, **Brömme D**, **Buttle DJ**, **Croucher LJ**, **Hollander AP**. Human cathepsin K cleaves native type I and II collagens at the N-terminal end of the triple helix. *Biochem J*. 1998;331 (Pt 3)(Pt 3):727–732.
7. **Christensen J**, **Shastri VP**. Matrix-metalloproteinase-9 is cleaved and activated by cathepsin K. *BMC Res Notes*. 2015;8:322.
8. **Costa AG**, **Cusano NE**, **Silva BC**, **Cremers S**, **Bilezikian JP**. Cathepsin K: its skeletal actions and role as a therapeutic target in osteoporosis. *Nat Rev Rheumatol*. 2011;7(8):447–456.
9. **Lee MH**, **Murphy G**. Matrix metalloproteinases at a glance. *J Cell Sci*. 2004;117(Pt 18):4015–4016.
10. **Lee MH**, **Rapti M**, **Murphy G**. Unveiling the surface epitopes that render tissue inhibitor of metalloproteinase-1 inactive against membrane type 1-matrix metalloproteinase. *J Biol Chem*. 2003;278(41):40224–40230.
11. **Amour A**, **Slocombe PM**, **Webster A**, **et al**. TNF-alpha converting enzyme (TACE) is inhibited by TIMP-3. *FEBS Lett*. 1998;435(1):39–44.
12. **Schon J**, **Chahla J**, **Paudel S**, **et al**. Expression profile of matrix metalloproteinases in the labrum of femoroacetabular impingement. *Bone Joint Res*. 2020;9(4):173–181.
13. **Lee M-H**, **Maskos K**, **Knäuper V**, **Dodds P**, **Murphy G**. Mapping and characterization of the functional epitopes of tissue inhibitor of metalloproteinases (TIMP)-3 using TIMP-1 as the scaffold: a new frontier in TIMP engineering. *Protein Sci*. 2002;11(10):2493–2503.
14. **Lee M-H**, **Rapti M**, **Knaüper V**, **Murphy G**. Threonine 98, the pivotal residue of tissue inhibitor of metalloproteinases (TIMP)-1 in metalloproteinase recognition. *J Biol Chem*. 2004;279(17):17562–17569.
15. **Asagiri M**, **Sato K**, **Usami T**, **et al**. Autoamplification of NFATc1 expression determines its essential role in bone homeostasis. *J Exp Med*. 2005;202(9):1261–1269.
16. **Balkan W**, **Martinez AF**, **Fernandez I**, **Rodriguez MA**, **Pang M**, **Troen BR**. Identification of NFAT binding sites that mediate stimulation of cathepsin K promoter activity by RANK ligand. *Gene*. 2009;446(2):90–98.
17. **Hawkes SP**, **Li H**, **Taniguchi GT**. Zymography and reverse zymography for detecting mmps and timps. *Methods Mol Biol*. 2010;622:257–269.
18. **Zalli D**, **Neff L**, **Nagano K**, **et al**. The actin-binding protein cofilin and its interaction with cortactin are required for podosome patterning in osteoclasts and bone resorption in vivo and in vitro. *J Bone Miner Res*. 2016;31(9):1701–1712.
19. **Toth M**, **Chvyrkova I**, **Bernardo MM**, **Hernandez-Barrantes S**, **Fridman R**. Pro-MMP-9 activation by the MT1-MMP/MMP-2 axis and MMP-3: role of TIMP-2 and plasma membranes. *Biochem Biophys Res Commun*. 2003;308(2):386–395.
20. **Jiang B**, **Liu J**, **Lee MH**. Targeting A designer TIMP-1 to the cell surface for effective MT1-MMP inhibition: A potential role for the prion protein in renal carcinoma therapy. *Molecules*. 2019;24(2):E255.
21. **Jiang B**, **Xu Y**, **Zhang Y**, **Lee MH**. Translocating a high-affinity designer TIMP-1 to the cell membrane for total renal carcinoma inhibition: Putting the prion protein to good use. *Mol Cell Biol*. 2019;39(18):e00128-19.
22. **Dai R**, **Wu Z**, **Chu HY**, **et al**. Cathepsin K: the action in and beyond bone. *Front Cell Dev Biol*. 2020;8:433.
23. **Ljusberg J**, **Wang Y**, **Lång P**, **et al**. Proteolytic excision of a repressive loop domain in tartrate-resistant acid phosphatase by cathepsin K in osteoclasts. *J Biol Chem*. 2005;280(31):28370–28381.
24. **Park JH**, **Lee NK**, **Lee SY**. Current understanding of RANK signaling in osteoclast differentiation and maturation. *Mol Cells*. 2017;40(10):706–713.
25. **Hotokezaka H**, **Sakai E**, **Kanaoka K**, **et al**. U0126 and PD98059, specific inhibitors of MEK, accelerate differentiation of RAW264.7 cells into osteoclast-like cells. *J Biol Chem*. 2002;277(49):47366–47372.
26. **Yi T**, **Kim H-J**, **Cho J-Y**, **et al**. Tetraspanin CD9 regulates osteoclastogenesis via regulation of p44/42 MAPK activity. *Biochem Biophys Res Commun*. 2006;347(1):178–184.

27. **Sundaram K**, **Nishimura R**, **Senn J**, **Youssef RF**, **London SD**, **Reddy SV**. RANK ligand signaling modulates the matrix metalloproteinase-9 gene expression during osteoclast differentiation. *Exp Cell Res.* 2007;313(1):168–178.
28. **Kim JH**, **Kim N**. Regulation of NFATc1 in osteoclast differentiation. *J Bone Metab.* 2014;21(4):233–241.
29. **Kim K**, **Lee SH**, **Ha Kim J**, **Choi Y**, **Kim N**. NFATc1 induces osteoclast fusion via up-regulation of Atp6v0d2 and the dendritic cell-specific transmembrane protein (DC-STAMP). *Mol Endocrinol.* 2008;22(1):176–185.
30. **Asagiri M**, **Takayanagi H**. The molecular understanding of osteoclast differentiation. *Bone.* 2007;40(2):251–264.
31. **Fitzgerald J**. Applications of CRISPR for musculoskeletal research. *Bone Joint Res.* 2020;9(7):351–359.

Author information:
- Y. Zhang, MSc, PhD Student
- B. Jiang, MSc, Senior Lab Technician
- P. Zhang, MSc, PhD Student
- M. H. Lee, DPhil, Senior Associate Professor
  Department of Biological Sciences/Academy of Pharmacy, Xi'an Jiaotong-Liverpool University, Suzhou, China.
- S. K. Chiu, PhD, Chief Scientific Officer, Shanghai XP Biomed Ltd, Shanghai, China.

Author contributions:
- Y. Zhang: Conceptualization, Methodology, Investigation, Formal analysis.
- B. Jiang: Project administration, Resources.
- P. Zhang: Investigation, Formal analysis.
- S. K. Chiu: Conceptualization, Methodology, Formal analysis, Writing – original draft, Writing – review & editing.
- M. H. Lee: Conceptualization, Methodology, Formal analysis, Writing – original draft, Writing – review & editing.

- Y. Zhang and B. Jiang are joint first authors.

Funding statement:
- The authors disclose receipt of the following financial or material support for the research, authorship, and/or publication of this article: the work is funded by the Key Program Special Fund (grant KSF-E-11), Suzhou.

ICMJE COI statement:
- Y. Zhang, B. Jiang, P. Zhang, S. K. Chiu, and M. H. Lee declare no conflict of interest.

Data sharing:
- T1PrαTACE is patent-protected (Chinese Intellectual Property Office Patent number 201810004200.2).

Acknowledgements:
- We would like to thank Suzhou KSF fund (KSF-E-11) for the generous funding of this project.

Open access funding
- The open access fee for this study was funded by the Key Program Special Fund (grant KSF-E-11).